Partially filled stripes in the two-dimensional Hubbard model: Statics and dynamics

E. Louis,[1] F. Guinea,[2] M. P. López Sancho,[2] and J. A. Vergés[2]
[1]*Departamento de Física Aplicada and Unidad Asociada of the Consejo Superior de Investigaciones Científicas (CSIC), Universidad de Alicante, Apartado 99, E-03080 Alicante, Spain*
[2]*Instituto de Ciencia de Materiales de Madrid, CSIC, Cantoblanco, E-28049 Madrid, Spain*
(Received 9 March 2001; revised manuscript received 19 June 2001; published 6 November 2001)

The internal structure of stripes in the two-dimensional Hubbard model is studied by going beyond the Hartree-Fock approximation. Partially filled stripes with inhomogeneous magnetization and charge along the stripe core, consistent with experimental observations, are stabilized by quantum fluctuations, included through the configuration interaction method. Similar configurations result to be stable for filled stripes, and have a lower energy than the standard paramagnetic core solution. Away from half-filling, solitonlike solutions show up within the Hartree-Fock approximation. The hopping of short regions of the stripes in the transverse direction is comparable to the bare hopping element. The hole-hole correlation shows maxima along the stripe direction, while the integrated value of $n_{\vec{\mathbf{k}}}$ compares satisfactorily with experimental results.

DOI: 10.1103/PhysRevB.64.205108 PACS number(s): 71.10.Fd, 71.30.+h

I. INTRODUCTION

By now it is well established that charged stripes are formed in a significant doping range of cuprate oxides.[1–3] The existence of these stripes was predicted, on the basis of mean-field calculations, in advance of its observation, both in the one-band[4–7] and the three-band Hubbard models.[8] This is one of the very few theoretical results in the field of high-T_c superconductivity which was confirmed after its prediction. However, experiments showed that stripes contained one hole per two sites of the stripe core (half-filled stripes), instead of one hole per site (filled stripes), as predicted by the Hartree-Fock calculations. Interest in these calculations decreased, as it was generally understood that the Hartree-Fock (HF) approximation was unable to obtain ground-state solutions which could be interpreted in terms of partially filled stripes. It must be noted, however, that the Hartree-Fock approximation, as analyzed in Ref. 9, can lead to self-consistent partially filled stripes, among a wide variety of other solutions which break translational invariance[7] (also see Sec. III A). These solutions are, at best, metastable solutions.[9] Alternatively, half-filled stripes can be stabilized by adding additional interactions to the Hubbard Hamiltonian.[10] Unrelated calculations found stripes with different fillings in the t-J model,[11] and, using different techniques, in the Hubbard model,[12] although other numerical calculations show conflicting results.[13,14] It was also argued that stripes in doped Mott antiferromagnets arise from a tendency toward phase separation, frustrated by electrostatic interactions.[15,16] Stripes in the Hubbard model have also been analyzed within slave-boson techniques, which use the HF solutions as input.[17] Extensions of the Hartree-Fock method which include low-energy spin and charge fluctuations (the random-phase approximation) were also discussed.[18]

In the present work, we analyze stripes in the one-band Hubbard model by extending the Hartree-Fock approximation by means of the configuration interaction (CI) method. The scheme was already presented in Refs. 19 and 20. The model is briefly discussed in Sec. II. Mean-field solutions for filled and partially filled stripes are analyzed in Sec. III. Some comments on configurations that may appear when holes are added to half-filled stripes are also made. The results beyond the Hartree-Fock method are presented in Sec. IV, where observable quantities such as the hole-hole correlations and the quasiparticle momentum dependence are also discussed. Section V resumes the main conclusions.

II. MODEL AND METHODS

Here we show that mean-field calculations, initially used to demonstrate the existence of stripes, can be improved in order to study the partially filled stripes observed experimentally. In addition, they provide significant insight into the internal structure of the stripes and their fluctuations in the transverse direction. The HF method can be viewed as a quasiclassical approximation to the spin and charge degrees of freedom. Their low-amplitude quantum fluctuations can be incorporated by using the random-phase approximation.[18] Finally, one needs to consider quantum tunneling processes between degenerate, or nearly degenerate, HF solutions, when there are many. This is achieved with the configuration interaction method, widely used in quantum chemistry.[19,20] The combination of HF and CI methods gives reasonable results even when applied to one dimensional systems.[22] The CI method restores the symmetries broken at the HF level, and provides information on the quantum dynamics of static HF solutions, which can be broadly classified into spin polarons or stripes.

The Hamiltonian is defined on a square lattice as

$$\mathcal{H}=t\sum_{i,jnn;s} c^{\dagger}_{i,s}c_{j,s}+U\sum_{i} n_{i,\uparrow}n_{i,\downarrow}, \tag{1}$$

where $n_{i,s}=c^{\dagger}_{i,s}c_{i,s}$, and the label i denotes a given site in a finite cluster. The usual mean-field decoupling of the interaction term is performed,

$$Un_{i,\uparrow}n_{i,\downarrow}=\frac{U}{4}(\langle q_i\rangle\hat{q}_i-\langle\vec{s}_i\rangle\hat{\vec{s}}_i) \tag{2}$$

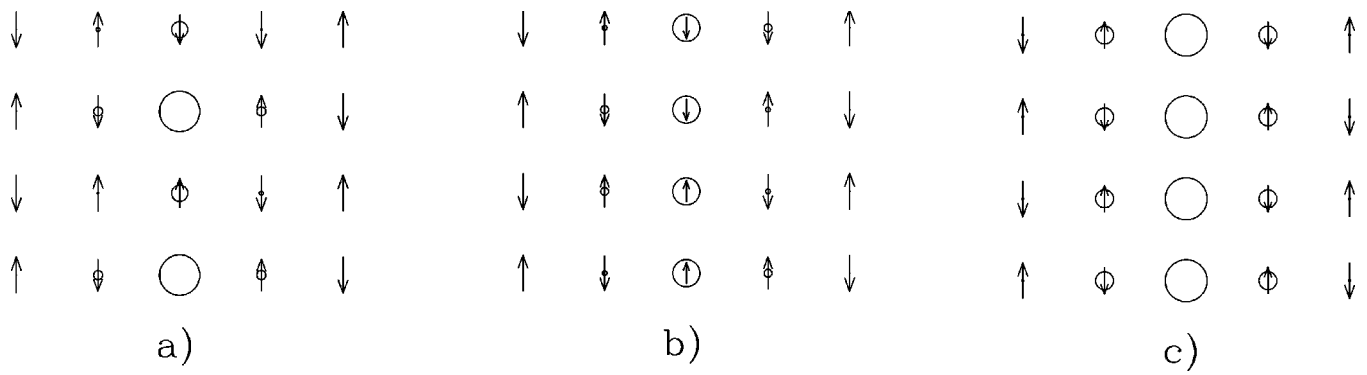

FIG. 1. Spin and charge textures for the three stripe solutions discussed in the text. Solutions (a) and (b) correspond to half-filled stripes, while solution (c) is a filled stripe. Hereafter we choose x and y axes to be the the horizontal and vertical axes, respectively.

where $\hat{q}_i=\Sigma_s c^\dagger_{i,s}c_{i,s}$ and $\hat{\vec{s}}_i=\Sigma_{s,s'}c^\dagger_{i,s}\vec{\sigma}_{s,s'}c_{i,s'}$ and $\vec{\sigma}$ is a vector made up of the three Pauli matrices. The Hartree-Fock equations are iterated until self-consistency. Calculations were carried out on $l\times m$ clusters with periodic boundary consitions. A thorough discussion of how the CI method is implemented, and of the way expected values are calculated, can be found in Refs. 19 and 20.

The choice of Slater determinants to be included in the configuration interaction method needs to take into account the fact that, at the mean-field level, there are many degenerate solutions[20] which are not orthogonal. When a given Slater determinant is included, all other solutions related to it by a lattice translation are also included. This procedure restores the translational symmetry broken at the mean-field level, as discussed above. In this respect, the scheme used here differs from the ordinary implementation of the CI method to nondegenerate atoms or molecules, where the usual choice is a set of Slater determinants built up of electron-hole pairs above the ground state. HF solutions having different energies and different charge and spin configurations have also been included in the CI calculation (see below). The number of possible configurations grows rapidly with the cluster size, posing a limitation on the maximum cluster size which can be studied within this method. The efficiency of this approach was checked in several studies of the Hubbard model in one and two dimensions,[19,20,22] and is further illustrated in the Appendix.

III. MEAN-FIELD SOLUTIONS

A. Filled and half-filled stripes

Different stripe solutions can be obtained by judiciously choosing the initial spin and charge texture. As extensively discussed elsewhere, previous mean-field studies focused on filled stripes,[7] which tend to be the solutions with the lowest energy per hole within this approximation, especially for the values of $U/t\sim 4$ used in the initial studies.[4–7]

There are, however, self-consistent solutions which describe partially filled stripes. These solutions have energies per hole comparable to those of the filled stripes for $U/t\sim 8-20$. They have a unit cell, along the stripe direction, which contains four sites. We have found two types of half-filled stripes: a solution with uniform charge and a $\uparrow\uparrow\downarrow\downarrow$ spin structure, and a solution with a charge density wave of period 2, and a $\uparrow 0\downarrow 0$ spin structure (see the Appendix). In both cases, a four-site periodicity along the stripe is found, which leads to a gap in the electronic spectrum. This is consistent with the well known instability of one-dimensional systems at the HF level.[21]

Typical stripe solutions obtained in this work, within the mean, field approximation and periodic boundary conditions, are shown in Fig. 1, where, for simplicity, we show results obtained in a 5×4 cluster, and $U=8$ (hereafter we shall use t as the unit of energy). The filled stripe, like the ones considered in previous mean-field calculations, is shown in Fig. 1(c), while Figs. 1(a) and 1(b) correspond to half-filled stripes, not reported earlier to our knowledge. We note that solutions similar to those of Fig. 1(a) and 1(b) can also be stable for the filled stripe (their stability depending on U). In this case, however, there are some differences with respect to the solutions of Fig. 1 that are worth noting (i) a large fraction of the charge is localized at sites neighboring the stripe core, and (ii) the spin arrangement at those sites is not as in the antiferromagnetic (AF) background; instead there are many sites ferromagnetically coupled. Textures such as those of Fig. 1 correspond to self-consistent Hartree-Fock solutions, and can be found in clusters of any size. A generalization of the $\uparrow\uparrow\downarrow\downarrow$ solution to a 16×16 cluster with 1/8 holes per site (32 holes) is shown in Fig. 2. The configuration is similar to pattern c of Table I, and, though the vector that separates two parallel stripes is $\mathbf{r}=(4a,0)$, the periodicity of the configuration is $8a$ in the x direction and $4a$ in the y direction.

We have also calculated the energy required to create a hole in these configurations by subtracting the energy of the AF background. The energies per hole obtained in this way are shown in Fig. 3. It is interesting to note that the standard solution for the filled stripe (nonmagnetic) is the best unrestricted Hartree-Fock (UHF) solution only for U smaller than $\approx 5t$. For larger values of the interaction parameter the non homogeneous solution of Fig. 1(b) becomes far more favorable. For large U the paramagnetic core solution has also higher energy than that of Fig. 1(a).

B. Nonconmensurate stripe solutions

Doping of stripes away from half-filling leads to the formation of defects. The addition of a single electron can in-

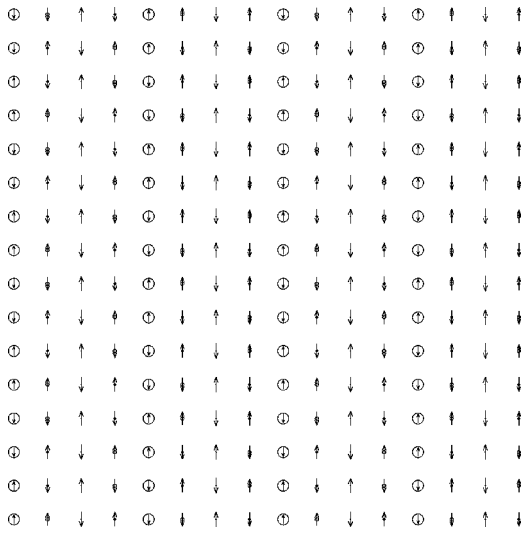

FIG. 2. Spin and charge textures for a 16×16 cluster with 32 holes ($\delta=1/8$, where δ is the number of holes per site) and $U/t=8$.

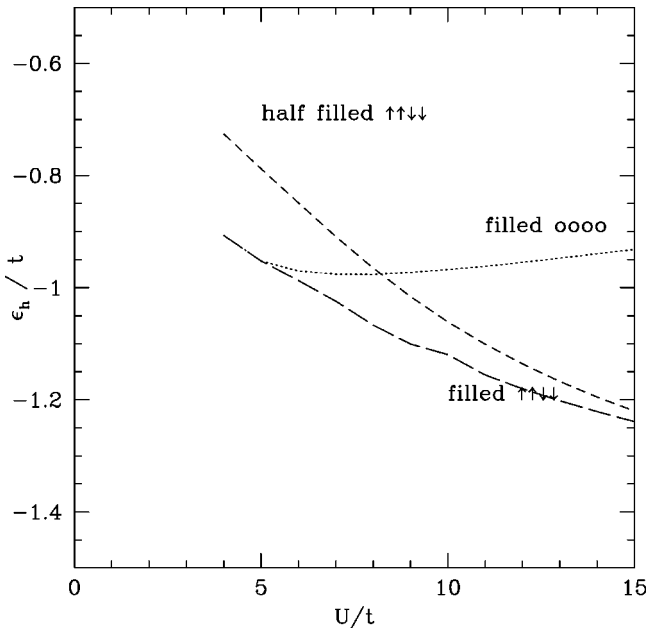

FIG. 3. Hartree-Fock energies per hole for filled and half-filled stripes as a function of U/t. The results correspond to 5×16 clusters with periodic boundary conditions.

duce the formation of two charge 1/2 solitons, or to the formation of steps. These mean-field solutions are shown in Fig. 4.

Charge fractionalization can be described within mean-field methods,[23] and leads to a description of the doped stripe as a Luttinger liquid[24] (also see Ref. 25). We find that steps are slightly more stable, in line with the arguments presented in Ref. 26. Note, however, that the step shown in Fig. 4 carries a unit of charge.

IV. RESULTS

A. Choice of configurations

We now hybridize the solutions described in Sec. III to construct better solutions of the Hubbard Hamiltonian, following the techniques explained in Ref. 20. Note that the stabilization of stripe solutions, within other schemes, requires a careful fine tuning of the boundary conditions,[11] leading to difficulties when comparing to solutions obtained for clusters with periodic boundary conditions.[13] Our method, on the other hand, gives solutions appropiate to clusters with periodic boundary conditions, but with built-in stripe correlations. Finally, to the basis set required to implement the CI we have added method solutions, which are slightly higher in energy. In Table I, we show different two-stripe configurations obtained within the Hartree-Fock method, and the energy gain from hybridizing those related by lattice translations. Results are also given for two filled stripes. As noted above, paramagnetic (homogeneous) solutions are far less favorable than nonhomogeneous solutions for the intermediate U of Table I. The additional gain associated by combining solutions not related by lattice translations is shown in Table II. We have checked that other textures, not depicted, do not change the results appreciably. The energy per hole, calculated by subtracting the HF energy of the antiferromagnetic solution for one electron per lattice site, results to be slightly more favorable for the half-filled

TABLE I. Energies of two stripes in 8×4 clusters for various Hartree-Fock solutions of filled (f) and half-filled (hf) stripes, and the CI combinations made by including all configurations related by lattice translations. The second row gives a sketch of the spin texture in the stripes ($U/t=8$). In the case of filled stripes, configuration *a* has a nonuniform charge along the stripe. Note that some configurations do not exist for either filled or half-filled stripes.

	a	*b*	*c*	*d*	*e*	*f*
	↑ ↑	↑ ↑	↑ ↓	0 0	0 0	0 0
	↑ ↑	↑ ↓	↑ ↓	↑ ↑	↑ ↓	0 0
	↓ ↓	↓ ↓	↓ ↑	0 0	0 0	0 0
	↓ ↓	↓ ↑	↓ ↑	↓ ↓	↓ ↑	0 0
E^f_{HF}	−23.431	–	–	−23.491	−23.373	−22.488
E^f_{CI}	−23.669	–	–	−23.697	−23.600	−23.050
E^{hf}_{HF}	−18.822	−18.824	−18.818	−18.689	−18.690	–
E^{hf}_{CI}	−19.438	−19.452	−19.437	−19.334	−19.334	–

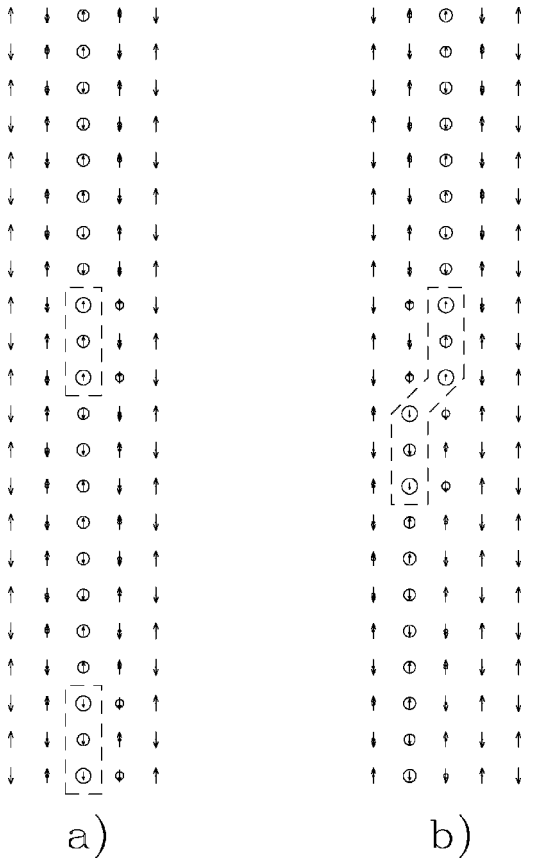

FIG. 4. Addition of a single hole to a half-filled stripe. Hartree-Fock spin and charge textures calculated for a 5×22 cluster with periodic boundary conditions and 12 holes ($U/t=8$). (a) Two-kink solution. (b) Step solution.

stripe, namely, -1.213 and -1.286 for the filled and half-filled stripes, respectively. However, the energy difference should be considered too small, particularly if one notes that the number of configurations included in the calculation is higher in the case of the half-filled stripes.

B. Size dependence and quantum dynamics of the stripes

The solutions obtained within the CI scheme restore translational symmetry, and can be classified according to the total momentum, which corresponds to the sum of the momenta of all electrons. The number of allowed momenta is given by the number of inequivalent displaced solutions which can be hybridized to build the trial wave function. This number is bound by the periodicity of each stripe along the longitudinal direction, and the distance between stripes with the same structure in a direction pependicular to the stripes.

TABLE III. Band energies of single stripes with different lengths. The results were obtained by including the HF configuration of Fig. 1(b) plus the configuration derived from it through a (0,1) displacement of the stripe core. The results correspond to $U/t=8$.

	4×5	8×5	12×5	16×5
E_{HF}	-11.24	-22.49	-33.734	-44.991
$E_{(0,0)}$	-12.41	-22.93	-33.958	-45.087
$E_{(\pi,0)}$	-10.98	-22.75	-33.939	-45.086
$E_{(0,\pi)}$	-10.76	-22.55	-33.749	-44.992

The difference in energies between solutions with different momenta reflects the energy gain from the delocalization of the Hartree-Fock solutions, which, in the present case, is associated with the quantum dynamics of the stripes. In the situations studied here, the ground state corresponds to the zero momentum solution.

In Tables III and IV we report the CI energies $E_{\mathbf{k}}$ at some symmetry points within the Brillouin zone, for one- or two-stripe solutions in clusters of increasing length. In the case of one stripe the CI results were obtained by including two UHF configurations, namely, that of Fig. 1(b) plus the one derived from it through a (0,1) displacement of the stripe core; for two stripes, configurations *a* and *c* of Table I were included. In both cases all configurations obtained by all lattice traslations from the original ones were also included. The UHF energies of the configurations included in the CI calculation are also shown in the tables. The results illustrate the size dependence of the CI energies. The energy gain decreases as the length of the stripe increases, due to the reduction in the overlap between solutions at different positions. Alternatively, one can say that transverse fluctuations of stripe segments are suppressed as the length of the segment increases. It is worth noting that the energy gain $E_{(0,0)}-E_{UHF}$ decreases faster, with the cluster size, in the two-stripe solutions than in the one stripe solution. This can be easily understood by recalling that a large part of that gain is kinetic energy, and thus it is easier for a smaller distortion of the AF background to move.

The bandwidths of the spectra obtained within the CI method are also plotted in Fig. 5. The CI calculation was carried out by including all configurations discussed in Table II. The results shown in Fig. 5 were fitted by means of $W=W_0e^{-l/l_0}$, where W_0 and l_0 are adjustable parameters. The

TABLE II. Energies obtained by hybridizing different solutions, sketched in Table I, in a 8×4 cluster. The last column shows the result obtained when including all configurations (the total number of different configurations obtained by lattice traslations is given in parentheses).

	$a+b$	$a+c$	$a+d$	$a+e$	$b+c$	$a-f$
E_{CI}^{f}	–	–	-24.116	-24.062	–	-24.551 (104)
E_{CI}^{hf}	-19.751	-19.940	-19.501	-19.840	-19.746	-19.991 (160)

TABLE IV. Band energies of clusters with two stripes of different length. The results correspond to $U/t=8$, and were obtained by including configurations *a* and *c* of Table I (HF energies of those configurations are also given).

	4×8	8×8	12×8	16×8	20×8
E^a_{HF}	-18.822	-37.57	-56.37	-75.160	-93.95
E^c_{HF}	-18.818	-37.58	-56.38	-75.166	-93.96
$E_{(0,0)}$	-19.94	-37.75	-56.41	-75.17	-93.96
$E_{(\pi,0)}$	-18.19	-37.57	-56.37	-75.17	-93.96
$E_{(0,\pi)}$	-18.20	-37.57	-56.37	-75.17	-93.96

values that we find are $(W_0,l_0)=(19.2,1.7)$ and $(3.0,4.6)$ for the $(1,0)$ and the $(0,1)$ directions, respectively. Note that the physical bandwidth cannot be defined in clusters narrower than four lattice spacings. The bandwidth associated with the displacement of a stripe of this length is $1.8t$. The two stripe results in Fig. 5 (triangles) are fitted in the same way, with $(W_0,m_0)=(10.1,2.1)$. In this case the W bandwidths in the two directions almost coincide. The exponential suppression of the tunneling of stripe segments of increasing length is expected on general grounds.

The CI results discussed above suggests that the stabilization of half-filled stripes is a general result, at least for values of U/t in the range 6–20. The value $U/t=8$ corresponds to a t-J model with $J/t=1/2$. The energy per hole that we obtain compares well with calculations for this model.[27] For $U/t=12$ $(J/t=1/3)$, we obtain $\epsilon_h\approx-1.71\pm0.05t$. This value is also in reasonable agreement with other calculations.[28]

C. Charge correlations

We have also calculated the hole-hole correlation $C_{i,j}=\langle(1-n_i)(1-n_j)\rangle$ for a half-filled stripe in a 5×4 cluster.

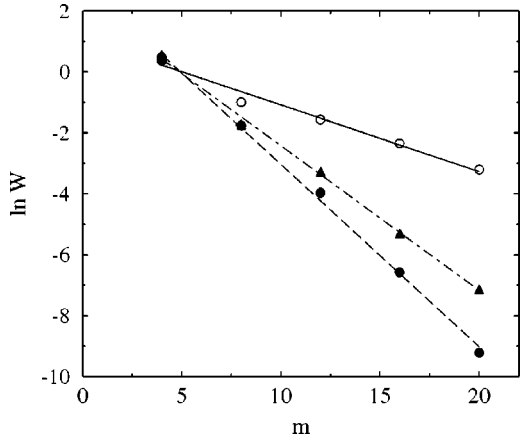

FIG. 5. Quasiparticle band width (W) in the directions $(0,0)\rightarrow(1,0)$ (filled circles) and $(0,0)\rightarrow(0,1)$ (empty circles) obtained on $5\times l$ clusters with a single half-filled stripe vs the stripe length l. Results for two stripes on $8\times l$ clusters are also shown (triangles).

The optimal CI wave function, discussed above, was used in the calculation. $C_{i,j}$ shows a maximum (0.021) when the holes are separated by a vector $\mathbf{r}_{ij}=\mathbf{r}_i-\mathbf{r}_j=(0,m)$, that is, when both are along the stripe direction. This feature of the hole-hole correlation differentiates stripes from other two hole configurations investigated within the t-J model[29] or the Hubbard model.[30,20] The results are shown in Table V. Note that the two main configurations involved, $(\uparrow\uparrow\downarrow\downarrow)$ and $(\uparrow0\downarrow0)$, can be viewed as a superposition of site-centered and bond-centered one-dimensional domain walls.[22] These configurations lead to a very accurate description of the dynamics of a hole in the one-dimensional Hubbard model[22] (also see the Appendix). The fact that the maximum hole-hole correlation is found along the stripe (see the discussion above) implies an additional similarity between the stripe solution and one-dimensional Luttinger liquids. Thus the stripes can be viewed as a one-dimensional system at quarter-filling.[31,32] Because of the commensuration with the lattice, we find a gap in the charge spectrum.[9] We estimate the value of this gap, Δ_{ch}, beyond mean-field theory, by calculating $\Delta_{ch}=E_{n_h+1}+E_{n_h-1}-2E_{n_h}$ around the optimal filling. For $U/t=8$, we obtain, $\Delta_{ch}=0.7\pm0.1t$, which is lower than the Hartree-Fock gap. For $U/t=12$, we find $\Delta_{ch}=0.5\pm0.1t$.

TABLE V. Hole-hole correlations $\langle(1-n_i)(1-n_j)\rangle$ for half-filled stripes on $l\times m$ clusters as a function of the vector $\mathbf{r}_{ij}$. The results correspond to $U=8t$, while the direction parallel to the stripe is $(1,0)$. A single stripe was included in 4×5 and 8×5 clusters, and two stripes in a 4×8 cluster. The $m\times5$ clusters ($m=4$ and 8) configuration of Fig. 1(b) and that obtained by displacing its core a lattice vector $(0,1)$ are used, while in the 4×8 cluster configurations *a* and *c* of Table I were included. In both cases the configurations derived by applying all lattice translations to the above-mentioned configurations were also included in the CI calculation.

$\mathbf{r}_{ij}/l\times m$	4×5	8×5	4×8
(0,0)	0.198	0.192	0.218
(1,0)	-2.05×10^{-2}	-1.99×10^{-2}	-1.95×10^{-2}
(2,0)	1.50×10^{-3}	1.77×10^{-3}	4.07×10^{-3}
(3,0)	–	–	1.25×10^{-2}
(4,0)	–	–	3.22×10^{-2}
(0,1)	-1.49×10^{-2}	-1.23×10^{-2}	-9.60×10^{-3}
(0,2)	2.16×10^{-2}	2.49×10^{-2}	2.93×10^{-2}
(0,3)	–	2.33×10^{-2}	–
(0,4)	–	2.63×10^{-2}	–
(1,1)	6.34×10^{-3}	4.93×10^{-3}	7.57×10^{-3}
(2,2)	2.01×10^{-3}	2.44×10^{-3}	4.80×10^{-3}
(3,3)	–	2.46×10^{-3}	–
(1,2)	6.02×10^{-3}	9.42×10^{-3}	8.64×10^{-3}
(2,1)	1.63×10^{-3}	1.35×10^{-3}	4.10×10^{-3}
(1,3)	–	9.55×10^{-3}	–
(3,1)	–	–	1.25×10^{-2}
(3,2)	–	–	1.25×10^{-2}
(1,4)	–	1.06×10^{-2}	–
(4,1)	–	–	3.22×10^{-2}
(4,2)	–	2.48×10^{-3}	3.22×10^{-2}

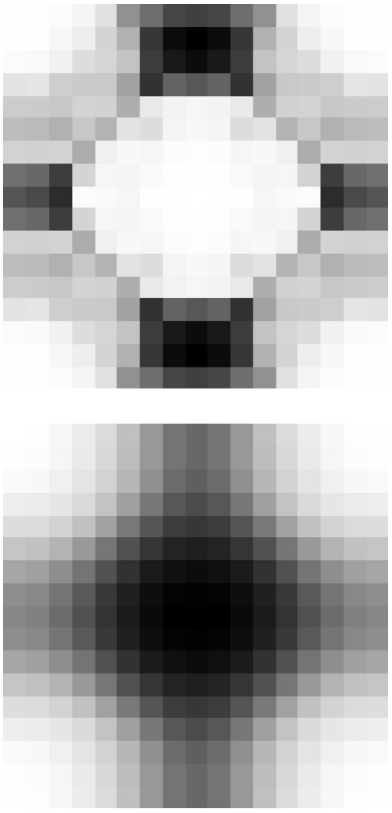

FIG. 6. Spectral weight $n_{\vec{\mathbf{k}}}$ integrated over either the highest 64 occupied electron states (upper) or the whole valence band (lower), for a 16×16 cluster with 224 electrons (32 holes). The results correspond to a stripe solution similar to configuration *c* of Table I with periodicities $8a$ and $4a$ in the *x* and *y* directions, respectively, like those of Fig. 2. The calculations were carried out for a cluster with periodic boundary conditions.

D. Quasiparticle momentum dependence

We have also computed the value of $n_{\vec{\mathbf{k}}}$ from the solutions described above. Figure 6 shows the spectral weight $n_{\vec{\mathbf{k}}}$ integrated over either the highest 64 occupied electron states (upper) or the whole valence band (lower). The results correspond to a 16×16 cluster with 224 electrons (32 holes) and periodic boundary conditions, and were obtained within the UHF approximation for a stripe solution similar to configuration *c* of Table I with periodicities $8a$ and $4a$ in the *x* and *y* directions, respectively (see Fig. 2). Although, as discussed below, the present results essentially agree with the most detailed experimental analyses of the electronic structure of stripe phases in cuprates,[33–35] a striking difference is worthy of comment: while in the experimental spectra of Ref. 35 the *x* and *y* directions are equivalent, in our calculations they are not (the spectra show a higher weight along the *y* direction as should correspond to the stripe configuration of Fig. 2). However, in a recent experimental study it was pointed out that most measurements were (and are) carried out on twinned crystals; thereby the apparent two-dimensional character observed in many cases (also note that Ref. 35 suggested the existence of two different domains with perpendicular stripes).

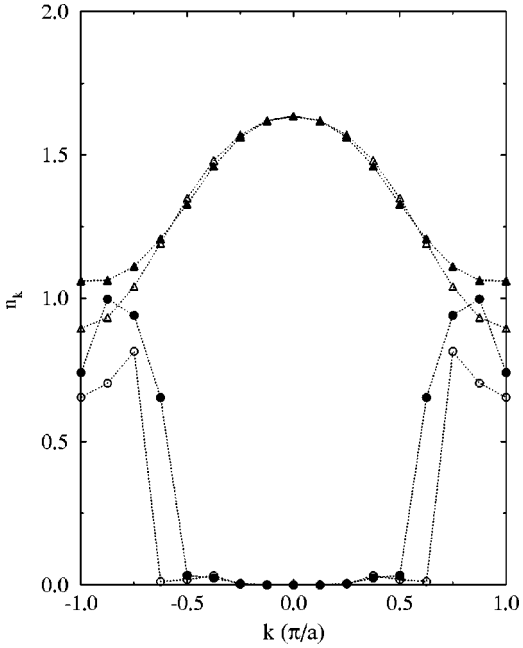

FIG. 7. Spectral weight $n_{\vec{\mathbf{k}}}$ integrated over either the highest 64 occupied electron states (upper) or the whole valence band (lower), along the $(k_x,0)$ (empty symbols) and $(0,k_y)$ (filled symbols) directions for the cluster and stripe solutions of Fig. 6.

Several features of the results, that agree with the experimental data, are worth of comment. The spectral weight at the center of the Brillouin zone mainly comes from electron states deep in the band. On the other hand, summing up the contribution of all electrons does not eliminates the strong anisotropy (the spectral weight is maximum along the *x* and *y* axis), as pointed out in Ref. 35 when commenting upon the results obtained after integrating over a 500 meV energy window of the Fermi level. In the experimental results the Fermi surface was placed at $k_x=\pm\pi/4$ or $k_x=\pm\pi/4$ lines for the two domains, respectively. This is compatible with the results shown in Fig. 6, as can be more clearly noted when plotting the spectral weight along the axes (see Fig. 7). The strong spectral weight around the zone center is no longer present when the contribution of deep electrons is not included. This is clearly visible in Fig. 6 and in Fig. 3 of Ref. 35 (also see Fig. 7). Now the spectral weight is concentrated near the points $(\pm\pi,0)$ and $(0,\pm\pi)$, and bounded by the lines mentioned above. We should note that this is found for a stripe pattern with an $8a$ periodicity in the *x* direction, significantly different from the configuration with a $4a$ periodicity proposed in Ref. 35, indicating that what matters is the distance between stripes and not subtle differences in spin and/or charge arrangements.

We have checked on smaller clusters that these results are not changed when going beyond UHF by means of the CI procedure. It is appealing that inhomogeneous spectral intensities are obtained even when charge and spin distributions are homogeneous in real space, as in the CI solutions proposed here.[36]

V. CONCLUDING REMARKS

We have shown that the half-filled stripes observed in experiments in cuprates can be derived using the same meth-

TABLE VI. CI and exact energies for two and four electrons ($N_h=2$ and 0, respectively) on a four-site chain with periodic boundary conditions (square) for two values of the electronic repulsion U. The weight of the included UHF configurations in the CI ground state is also given (note that, as the basis is not orthonormalized, weights can be larger than 1). The number of different configurations obtained from a given one through lattice translations is given in parentheses.

N_h	U	$\uparrow\downarrow\uparrow\downarrow$	0 0 0 0	$\uparrow$ 0 $\downarrow$ 0	$\uparrow\uparrow\downarrow\downarrow$	E_{CI}	E_{exact}
0	5	0.518 (2)	–	–	0.225 (4)	−1.795	−1.844
	10	0.557 (2)	–	–	0.268 (4)	−1.095	−1.100
2	5	–	41.88 (1)	79.62 (4)	69.46 (4)	−3.348	−3.348
	10	–	2.22 (1)	5.18 (4)	4.95 (4)	−3.149	−3.149

ods which lead to the prediction of the existence of (filled) stripes in the Hubbard model.[4–7] The CI method allows us to describe quantum transverse fluctuations of the stripes, which are significant (comparable to t) for segments of length of 4–6 lattice units. Hole-hole correlation shows maxima along the stripe direction. We present the distribution of $n_{\tilde{\mathbf{k}}}$, with good agreement with experimental results.

The usefulness of the present method for the study of half-filled stripes suggests that a detailed description of spin waves in the antiferromagnetic background is not essential.[37] On the other hand, the scheme used here shows that there is a delicate balance between spin polarons[7,20] and stripes, which seems also to be found in Monte Carlo calculations of the t-J model.[11,13,14,27,38] A detailed comparison of the relative stability of these phases cannot be done within the present method, and also seems difficult to achieve by other techniques. It would be interesting to analyze further the experimental implications of this near degeneracy of qualitatively different solutions.

Finally, the present method suggests that dynamic inhomogeneous spin and charge textures, like stripes or spin polarons, are closely related to the mean-field solutions. The existence of inhomogeneities in these solutions is related to the fact that translationally invariant wave functions, in the mean field, lead to states with a negative compressibility, which are unstable toward phase separation.[39]

ACKNOWLEDGMENTS

The financial support of the CICyT (Spain), through Grants Nos. PB96-0875, PB96-0085, 1FD97-1358 and BFM2000-1107, and CAM (Madrid), through Grant No. 07N/0045/98, is gratefully acknowledged.

APPENDIX: FOUR OR TWO ELECTRONS ON A SQUARE

In this appendix we discuss the ground-state energies for two or four electrons on a four-site chain with periodic boundary conditions (or, equivalently, a square). We note that this may represent up to some extent the core of the stripes in Fig. 1. The results are reported in Table VI. The CI calculation includes the UHF configurations of Fig. 1. The results indicate that while the weight of the paramagnetic configuration in the four-electron ground state is negligible, that of the configuration in Fig. 1(b) is quite important. This is in line with our UHF results for the filled stripe shown in Fig. 2, which indicate that the aforementioned configuration is by far more favorable than the paramagnetic core solution. The error in the energy for four electrons is less than 3%. In the case of two electrons, configurations (a) and (b) in Fig. 1 have a similar weight in the ground-state wave function. On the other hand, the exact energy is reproduced by the CI calculation only when the paramagnetic configuration is included. These results illustrate the use and support the efficiency of the nonstandard CI approach used in this work.

[1] S.-W. Cheong, G. Aeppli, T.E. Mason, H. Mook, S.M. Hayden, P.C. Canfield, Z. Fisk, K.N. Clausen, and J.L. Martínez, Phys. Rev. Lett. **67**, 1791 (1991).
[2] T.E. Mason, G. Aeppli, and H.A. Mook, Phys. Rev. Lett. **68**, 1414 (1992).
[3] J. Tranquada, B.J. Sternlieb, J.D. Axe, Y. Nakamura, and S. Uchida, Nature (London) **375**, 561 (1995).
[4] J. Zaanen and O. Gunnarsson, Phys. Rev. B **40**, 7391 (1989).
[5] D. Poilblanc and T.M. Rice, Phys. Rev. B **39**, 9749 (1989).
[6] H.J. Schulz, Phys. Rev. Lett. **64**, 1445 (1990).
[7] A.R. Bishop, F. Guinea, P.S. Lomdahl, E. Louis, and J.A. Vergés, Europhys. Lett. **14**, 157 (1991); J.A. Vergés, E. Louis, P.S. Lomdahl, F. Guinea, and A.R. Bishop, Phys. Rev. B **43**, 6099 (1991).
[8] J.A. Vergés, F. Guinea, and E. Louis, Phys. Rev. B **46**, 3562 (1992).
[9] J. Zaanen and A.M. Oleś, Ann. Phys. (Leipzig) **5**, 224 (1996).
[10] D. Góra, K. Rościszewski, and A.M. Oleś, Phys. Rev. B **60**, 7429 (1999).
[11] S.R. White and D.J. Scalapino, Phys. Rev. Lett. **80**, 1272 (1998).
[12] M. Fleck, A.I. Lichtenstein, E. Pavarini, and A.M. Oleś, Phys. Rev. Lett. **84**, 4962 (2000).
[13] C.S. Hellberg and R. Manousakis, Phys. Rev. Lett. **83**, 132 (1999).
[14] M. Calandra and S. Sorella, Phys. Rev. B **61**, R11894 (2000).
[15] V.J. Emery and S.A. Kivelson, in *Proceedings of the First Polish-U.S. Conference on High Temperature Superconductivity* (Springer-Verlag, New York, 1996).
[16] S. Caprara, C. Castellani, C. Di Castro, M. Grilli, A. Perali, and M. Sulpizi, Physica C **318**, 230 (1999).
[17] G. Seibold, E. Sigmund, and V. Hizhnyakov, Phys. Rev. B **57**, 6937 (1998).
[18] F. Guinea, E. Louis, and J.A. Vergés, Phys. Rev. B **45**, 4752 (1992).

[19] E. Louis, G. Chiappe, F. Guinea, J.A. Vergés, and E.V. Anda, Phys. Rev. B **48**, 9581 (1993).
[20] E. Louis, F. Guinea, M.P. López-Sancho, and J.A. Vergés, Europhys. Lett. **44**, 229 (1998); Phys. Rev. B **59**, 14005 (1999).
[21] Half-filled stripes with a homogeneous paramagnetic core, such as those reported in Ref. 10 (see Fig. 1 and Table I of that work) are not fully converged, self-consistent HF solutions. They only exist in the filled case (see Fig. 3 of the present work).
[22] M. Berciu and S. John, Phys. Rev. B **61**, 10 015 (2000).
[23] A.J. Heeger, S. Kivelson, W.P. Su, and J.R. Schrieffer, Rev. Mod. Phys. **60**, 781 (1988).
[24] G. Gómez-Santos, Phys. Rev. Lett. **70**, 3780 (1993).
[25] J. Zaanen, O.Y. Osman, and W. van Saarloos, Phys. Rev. B **58**, R11 868 (1998).
[26] M. Bosch, W. van Saarloos, and J. Zaanen, Phys. Rev. **63**, 092501 (2001).
[27] S.R. White and D.J. Scalapino, Phys. Rev. B **61**, 6320 (2000).
[28] S.R. White and D.J. Scalapino, Phys. Rev. Lett. **81**, 3227 (1998).
[29] J. Riera and E. Dagotto, Phys. Rev. B **57**, 8609 (1998).
[30] G. Fano, F. Ortolani, and A. Parola, Phys. Rev. B **42**, 6977 (1990).
[31] A. Castro-Neto and F. Guinea, Phys. Rev. Lett. **80**, 4040 (1998).
[32] A.L. Chernyshev, A.H. Castro-Neto, and A.R. Bishop, Phys. Rev. Lett. **84**, 4922 (2000).
[33] M. Ichioka and K. Machida, J. Phys. Soc. Jpn. **68**, 4020 (1999).
[34] M.G. Zacher, R. Eder, A. Arrigoni, and W. Hanke, Phys. Rev. Lett. **85**, 2585 (2000).
[35] X.J. Zhou, P. Bogdanov, S.A. Kellar, T. Noda, H. Eisaki, S. Uchida, Z. Hussain, and Z.-X. Shen, Science **286**, 268 (1999).
[36] A. Mook, P. Dai, F. Dogan, and R.D. Hunt, Nature (London) **404**, 729 (2000).
[37] The CI method allows for a systematic inclusion of spin fluctuations, by adding configurations in which the spins along a bond are flipped. We have checked that these configurations do not change the results qualitatively. Also see C. Buhler, S. Yunoki, and A. Moreo, Phys. Rev. Lett. **84**, 2690 (2000).
[38] G.B. Martins, C. Gazza, J.C. Xavier, A. Feiguin, and E. Dagotto, Phys. Rev. Lett. **84**, 5844 (2000).
[39] F. Guinea, E. Louis, M.P. López-Sancho, and J.A. Vergés, Solid State Commun. **113**, 593 (2000).